

Elastic and Photoelastic Properties of TeO₂ Single Crystal

Naoya Uchida and Yoshiro Ohmachi

Citation: *Journal of Applied Physics* **40**, 4692 (1969); doi: 10.1063/1.1657275

View online: <http://dx.doi.org/10.1063/1.1657275>

View Table of Contents: <http://scitation.aip.org/content/aip/journal/jap/40/12?ver=pdfcov>

Published by the AIP Publishing

Articles you may be interested in

[Photovoltaic effect in Bi₂TeO₅ photorefractive crystal](#)

Appl. Phys. Lett. **107**, 151905 (2015); 10.1063/1.4933097

[Structural, electronic, and optical properties of \$\alpha\$, \$\beta\$, and \$\gamma\$ -TeO₂](#)

J. Appl. Phys. **107**, 093506 (2010); 10.1063/1.3406135

[Elastic, dielectric, and piezoelectric properties of Ba_{0.5}TeMo_{0.5}O₉ single crystal](#)

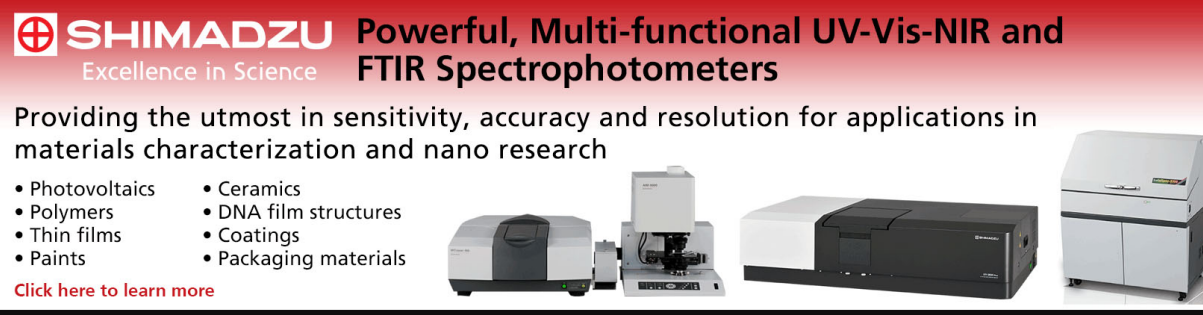
Appl. Phys. Lett. **93**, 252906 (2008); 10.1063/1.3055607

[Acoustic Attenuation in TeO₂](#)

J. Appl. Phys. **43**, 2915 (1972); 10.1063/1.1661627

[Temperature Dependence of Elastic, Dielectric, and Piezoelectric Constants in TeO₂ Single Crystals](#)

J. Appl. Phys. **41**, 2307 (1970); 10.1063/1.1659223

An advertisement for Shimadzu spectrophotometers. It features the Shimadzu logo (a red square with a white 'S') and the text 'SHIMADZU Excellence in Science' in white on a red background. To the right, the text 'Powerful, Multi-functional UV-Vis-NIR and FTIR Spectrophotometers' is written in black. Below this, a paragraph states: 'Providing the utmost in sensitivity, accuracy and resolution for applications in materials characterization and nano research'. A list of applications follows: Photovoltaics, Polymers, Thin films, Paints, Ceramics, DNA film structures, Coatings, and Packaging materials. At the bottom left, a red link says 'Click here to learn more'. On the right, four different Shimadzu spectrophotometer models are shown: a small benchtop unit, a larger benchtop unit with a sample holder, a large floor-standing unit, and a very large floor-standing unit with a sample compartment.

Elastic and Photoelastic Properties of TeO₂ Single Crystal

NAOYA UCHIDA AND YOSHIRO OHMACHI

Electrical Communication Laboratory, Nippon Telegraph and Telephone Public Corporation, Musashino, Tokyo, Japan

(Received 26 May 1969; in final form 22 September 1969)

Elastic stiffness, acoustic absorption, and photoelastic constants of the crystal have been determined at room temperature using ultrasonic light diffraction and pulse-echo methods. Two acoustic modes have been found to be particularly useful to acousto-optical applications: One is the shear mode propagated in the $[110]$ direction with displacement along $[\bar{1}10]$, which is characterized by a remarkably high acousto-optical figure of merit, $M(n^6 p^2 / \rho v^3) = 793 \times 10^{-18} \text{ sec}^3/\text{g}$; and the other is the longitudinal mode along $[001]$ with high figure of merit defined taking account of frequency bandwidth, $M'(n^7 p^2 / \rho v) = 142 \times 10^{-7} \text{ cm}^2 \cdot \text{sec}/\text{g}$, and low acoustic loss.

INTRODUCTION

Several applications of light-sound interaction, Debye-Sears effect^{1,2} and Bragg deflection,³ have been proposed for acoustooptical devices such as light modulators,^{4,5} deflectors,⁶⁻⁹ delay lines,¹⁰ and some other signal processors.^{11,12} Performance of such devices entirely depend upon acoustic, optical, and acousto-optical properties of constituent medium elements in which light and sound interact with each other. Furthermore, for the development of practical devices, high efficiency in the interaction, low acoustic loss, and temperature stability are required for the medium-elements as well as high optical quality and availability of large size elements.

Although a number of solid materials including crystalline and amorphous states have been surveyed by several authors¹³⁻¹⁶ and some of them are considered as suitable for the devices, increasing effort seems to be necessary to find the best materials. From the viewpoint mentioned above, basic aspects of acoustic and acousto-optical properties are investigated in paratellurite (TeO₂) single crystal which was first studied by Arlt

and Schweppe,¹⁷ for its elastic, piezoelectric, dielectric, and optical properties. Two remarkable facts were revealed by them in its elastic behavior; one is that c_{66} is larger than c_{11} , and the other is that an exceptionally slow shear wave is propagated in $\langle 110 \rangle$ directions. The latter feature, accompanied by high refractive indices of the crystal, immediately suggests that the crystal will serve for an acousto-optical device with high efficiency. In this paper, experimental results on elastic stiffness, acoustic absorption, and photoelastic constants are described and the applicability of the crystal for acousto-optical devices is briefly discussed.

EXPERIMENTAL PROCEDURES

Single crystals of TeO₂ were grown by the Czochralski method from a melt,^{17,18} and three kinds of specimens with different orientations were cut out of them. Each specimen was a rectangular solid in shape and was about 5 to 12 mm in size. One was oriented along the principle axes, the second had one edge along $[110]$ and the third had one edge along $[101]$. Measured density of the crystal was 5.99 and the value was in good agreement with the calculated one.¹⁹

Continuous and pulsed ultrasounds of 10 to 300 MHz were generated by quartz and LiNbO₃ transducers with various fundamental frequencies ranging from 10 to 60 MHz. Sound velocities were determined from distances between diffracted light spots. Photoelastic constants were measured using the technique developed by Dixon and Cohen,²⁰ in which the unknown constants of a specimen were determined relative to those of some standard material bonded to the specimen. A 6328 Å He-Ne laser was used as a light source. Measurements of acoustic absorption coefficients were made by pulse-echo method.

¹ P. Debye and F. W. Sears, Proc. Nat. Acad. Sci. (USA) **18**, 409 (1932).

² R. Lucas and P. Biquard, Compt. Rend. **194**, 2132 (1932).

³ L. Brillouin, Ann. Phys. (France) Ser. 9, **17**, 88 (1922).

⁴ H. V. Hance and J. K. Parks, J. Acoust. Soc. Amer. **38**, 14 (1965).

⁵ R. W. Dixon and E. I. Gordon, Bell System Tech. J. **46**, 367 (1967).

⁶ A. Korpel, R. Adler, P. Desmares, and T. M. Smith, IEEE J. Quantum Electron. **1**, 60 (1965).

⁷ A. Korpel, R. Adler, P. Desmares, and W. Watson, Proc. IEEE **54**, 1429 (1966).

⁸ E. G. H. Lean, C. F. Quate, and H. J. Shaw, Appl. Phys. Lett. **10**, 48 (1967).

⁹ N. Uchida and H. Iwasaki, Japan. J. Appl. Phys. **8**, 811 (1969).

¹⁰ M. J. Brienza and A. J. DeMaria, Appl. Phys. Lett. **9**, 312 (1966).

¹¹ L. B. Lambert, IRE Int. Conv. Rec. **10**, Pt. 6, 69 (1962).

¹² M. King, W. R. Bennett, L. B. Lambert, and M. Arm, Appl. Opt. **6**, 1367 (1967).

¹³ T. M. Smith and A. Korpel, IEEE J. Quantum Electron. **1**, 283 (1965).

¹⁴ R. W. Dixon, J. Appl. Phys. **38**, 5149 (1967).

¹⁵ J. Reintjes and M. B. Schulz, J. Appl. Phys. **39**, 5254 (1968).

¹⁶ D. A. Pinnow and R. W. Dixon, Appl. Phys. Lett. **13**, 156 (1968).

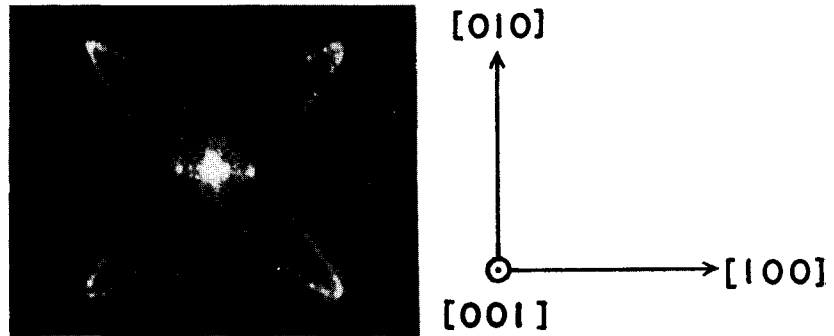
¹⁷ G. Arlt and H. Schweppe, Solid State Commun. **6**, 783 (1968).

¹⁸ N. Uchida, Y. Ohmachi, and N. Niizeki, Appl. Phys. Lett. (to be published).

¹⁹ H. Iwasaki and S. Miyazawa, Japan. J. Appl. Phys. (to be published).

²⁰ R. W. Dixon and M. G. Cohen, Appl. Phys. Lett. **8**, 205 (1966).

FIG. 1. Schaefer-Bergmann diffraction pattern for TeO_2 single crystal obtained by sound waves of 20 MHz.



According to the Raman-Nath²¹ and Rytow²² theories, diffracted light intensity of the first order I_1 relative to that of the zeroth order I_0 without acoustic field is proportional to sound power density when I_1 is sufficiently small. The maximum value of I_1 which satisfies the linear relation depends upon a value of the factor Q ($=K^2L/k$, where K and k represent sound and light wave numbers in a medium, respectively, and L is an interaction length),²³ and about $10^{-2}I_0$ is practically permissible in the worst case, that is, in the ideal Raman-Nath region. The present investigation of acousto-optical behaviors has been made under the condition that I_1 does not exceed the limit, and moreover under the condition that an incident angle is set so that the maximum I/I_0 is attained. Thus, in a combined system of TeO_2 and fused quartz rod used as a standard, the following relation holds among figure of merit M , relative diffracted light intensity I ($=I_1/I_0$) and generated sound power P ;

$$M_T = M_F (I_T^{(2)} I_T^{(3)} / I_F^{(1)} I_F^{(4)})^{1/2} (P_F / P_T), \quad (1)$$

where subscripts T and F stand for TeO_2 and fused quartz, respectively, and

$$M = n^6 p^2 / \rho v^3, \quad (2)$$

TABLE I. Elastic stiffness constants of TeO_2 at room temperature.

Constant	Present result ($\times 10^{11}$ dyn/cm ²)	Arlt <i>et al.</i> ¹⁷ ($\times 10^{11}$ dyn/cm ²)
c_{11}	5.32	5.6
c_{12}	4.86	5.16
c_{13}	2.12	2.72
c_{33}	10.85	10.51
c_{44}	2.44 ^a	2.70
c_{66}	5.52	6.68

^a Measured using pulse-echo method. Other values by ultrasonic light diffraction technique.

²¹ C. V. Raman and N. S. N. Nath, Proc. Indian Acad. Sci. **2A**, 406, 413 (1935).

²² S. M. Rytow, Phys. Z. Sowjet **8**, 626 (1935).

²³ G. W. Willard, J. Acoust. Soc. Amer. **21**, 101 (1949); see also, W. R. Klein and B. D. Cook, IEEE Trans. Sonics Ultrasonics **14**, 123 (1967).

in which n is the refractive index, p is the photoelastic constant, ρ is the density, and v is the sound velocity.¹³ The relative intensity $I_F^{(1)}$ is due to the outgoing acoustic pulse from a transducer cemented on a side of fused quartz and $I_F^{(4)}$ is due to the acoustic pulse first returning into the fused quartz through a bond after it is propagated in TeO_2 . The intensities $I_T^{(2)}$ and $I_T^{(3)}$ are due to the first outgoing pulse and that reflected from the free end in TeO_2 , respectively. The relative value of P was given by monitoring the input voltage E applied to the transducer, and I vs E^2 characteristics were always measured in order to increase the experimental accuracy. Equation (1) is a modification of that given by Dixon and Cohen,²⁰ and is useful when M_T/M_F is much different from unity. In general, differences of refractive indices and transparency of light between a sample and a standard material need not be taken into account as far as the ratio of the diffracted light intensity to that of the zeroth order, not the absolute intensity, is considered.²⁴

Paratellurite crystal belongs to the point group D_{12} ,²⁵ and possesses seven independent photoelastic constants; p_{11} , p_{12} , p_{13} , p_{31} , p_{33} , p_{44} , and p_{66} .²⁶ As the crystal is

TABLE II. Photoelastic constants of TeO_2 for an optical wavelength 6328 Å at room temperature.

Constant	Obtained value ^a
$ p_{11} $	0.0074
p_{12}	0.187
p_{13}	0.340
p_{31}	0.0905
p_{33}	0.240
p_{44}	~ -0.17
p_{66}	-0.0463

^a Only relative signs are given for all constants except p_{11} . Calculation indicates that the sign of p_{11} is probably the same as that of p_{12} , etc.

²⁴ Compare with Eq. (6b) given by Reintjes and Schulz in Ref. 15.

²⁵ R. W. G. Wyckoff, *Crystal Structure* (John Wiley & Sons, Inc., New York, 1963), Vol. 1, p. 255.

²⁶ J. F. Nye, *Physical Properties of Crystals* (Clarendon Press, Inc., Oxford, 1957), p. 251.

TABLE III. Calculated figures of merit in TeO₂.

Mode ^a	Acoustic wave		$v \times 10^{-6}$ (cm/sec)	Optical wave		Appropriate p_{ij}	Figures of merit	
	Propag.	Polar.		Propag.	Polar.		$M \times 10^{18}$ (sec ² /g)	$M' \times 10^7$ (cm ² sec/g)
L	[100]		2.98	[010]	[100]	p_{11}	0.048	0.097
L	[100]			[010]	[001]	p_{31}	10.6	22.9
L	[001]		4.26	[010]	[100]	p_{13}	34.5	142
L	[001]			[010]	[001]	p_{33}	25.6	113
S	[100]	[010]	3.04	[001]	arb.	p_{66}	1.76	3.70
L	[110]		4.21	$\bar{1}10$	[110]	$(p_{11} + p_{12} + 2p_{66})/2$	0.802	3.23
L	[110]			$\bar{1}10$	[001]	p_{31}	3.77	16.2
L	[101]		3.64	$\bar{1}01$	[010]	$(p_{12} + p_{13})/2$	33.4	101
L	[010]		2.98	$\bar{1}01$	[101]	$(p_{12} + p_{31})/2$	20.4	42.6
S	[110]	$\bar{1}10$	0.617	[001]	arb.	$(p_{11} - p_{12})/2$	793	68.6
S	[101]	$\bar{1}01$	2.08	[010]	[100]	$(p_{11} - p_{13})/2$	77.7	76.4

^a L stands for longitudinal mode and S for shear mode.

highly birefringent, p_{44} could not be independently determined in the experiment: for the shear wave with appropriate frequency higher than that available here was required for the light diffraction.²⁷ Unwanted distortion in the state of polarization occurred while the light traversed the thick specimen in the [001] direction, along which the crystal is highly optically active,¹⁷ perhaps due to residual strain and lineage structure¹⁹ (local misorientation of the crystal axes), and the use of the relevant direction was avoided except in case that the light was deflected by shear waves.

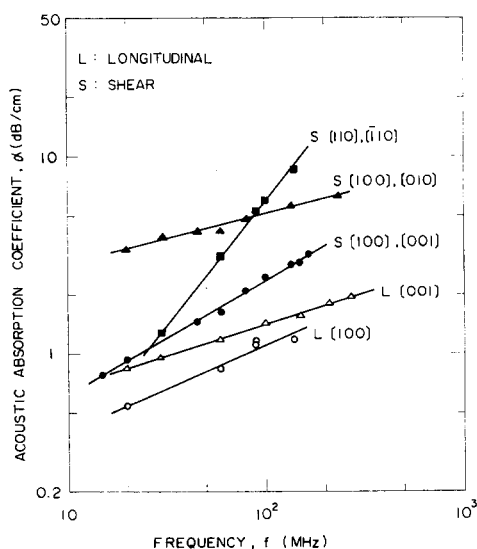


FIG. 2. Frequency dependence of acoustic absorption coefficients in TeO₂ for various sound modes at room temperature. Directions of propagation for longitudinal waves and those of propagation and polarization for shear waves are given in this figure.

²⁷ R. W. Dixon, IEEE J. Quantum Electron. **3**, 85 (1967).

EXPERIMENTAL RESULTS

Figure 1 shows a typical Schaefer-Bergmann diffraction pattern²⁸ obtained by sound waves of 20 MHz. The laser beam was incident upon the crystal along the (001) direction, while the sound waves were propagated in the (001) plane. Two spots deflected horizontally were due to a longitudinal wave along (100), of which velocity was 2.98×10^5 cm/sec. Butterfly-type contours produced by shear waves show two unusual behaviors

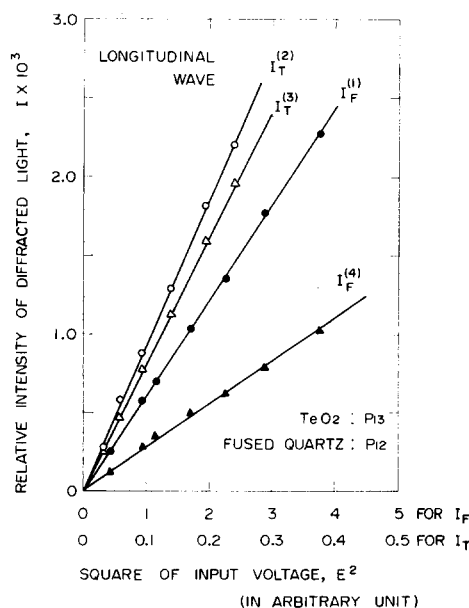


FIG. 3. Relations between relative intensity of the first order diffracted light and square of input voltage for combined system of TeO₂ and fused quartz.

²⁸ Cl. Schaefer and L. Bergmann, Naturwiss. **22**, 685 (1934).

pointed out by Arlt *et al.*¹⁷: exceptionally slow shear wave along (110), $v=0.617 \times 10^5$ cm/sec, and the fast shear wave along (100), $v=3.04 \times 10^5$ cm/sec, which is propagated a little faster than the longitudinal one.

Values of the elastic stiffness constants at room temperature were calculated from measured sound velocities and density ($\rho_{\text{meas}}=5.99$ g/cm³), and are listed in Table I. All velocities except that of the shear wave in the [001] direction were determined using ultrasonic light diffraction technique. As mentioned in the previous section, it required sound frequency higher than 0.5 GHz to produce the diffraction pattern using the shear wave concerned.²⁷ Values of c_{12} and c_{13} were obtained from the shear velocity along [110] (displacement along $[\bar{1}10]$) and that along [101] (displacement along $[\bar{1}01]$), respectively. The values obtained here are believed accurate to 2% except for c_{13} for which the accuracy is about 4%. Although the value c_{66} was reported to be remarkably larger than c_{11} by Arlt *et al.*,¹⁷ only a little difference is observed between them in the present experiment. On the other hand, velocity of the slowest shear wave along [110] is well confirmed.

Frequency dependence of the acoustic absorption coefficients α for several sound modes measured at room temperature are shown in Fig. 2. The coefficients for shear waves along [110] and [001] were given by Arlt *et al.*¹⁷ as about 1.3 and 1.1 dB/cm at 30 MHz, respectively, and are in good agreement with the present results. From the figure, values of γ in $\alpha \propto f^\gamma$ are determined and extend from 0.25 to 1.2 in the present frequency range. Attenuations of shear waves are generally larger than those of longitudinal ones at the frequency above 20 MHz.

Figures of merit M for an optical wavelength 6328 Å were measured at room temperature using the Dixon-Cohen method²⁰ for various combinations of the propagation and polarization directions of sound and light. A typical example of I vs E^2 characteristics is shown in Fig. 3. Diffracted intensities for TeO_2 and fused quartz are due to the pulsed longitudinal sound wave traveling in both media. Seven independent photoelastic components were determined using the method of least squares from fifteen values of M and are summarized in Table II. Values of M_F used here are 1.56×10^{-18} sec³/g for longitudinal wave (relevant photoelastic constant is p_{12}) and 0.444×10^{-18} sec³/g for shear wave [the component is $(p_{11}-p_{12})/2$].²⁹ The obtained values of the photoelastic constants are considered to be accurate to several percent except for p_{11} for which the accuracy is 50%. Although absolute signs cannot be determined by the ultrasonic method, several values of M in the oblique-cut specimens served to decide the relative signs for all components except p_{11} . Present calculation clearly indicates that four components p_{12} , p_{13} , p_{31} , and p_{33} have the same

sign, while the sign of p_{44} and p_{66} is opposite to the former one. The calculation also suggests that the sign of p_{11} is probably the same as that of p_{12} , etc. The ratio p_{12}/p_{11} is found to be especially large as a result of small p_{11} , and the behavior somewhat resembles that of rutile.^{14,15}

Table III lists the calculated figures of merit M and M' ($=n^2 p^2 / \rho v$) for several directions using the obtained photoelastic constants. The latter figure of merit M' is defined by Gordon³⁰ taking account of frequency bandwidth as well as the diffracted light intensity. The highest value of M is attained for the slowest shear wave along [110] and is about 6 times as large as that of water.²⁸ As shown in Fig. 1,^{29,31} a large variation in the diffracted light intensity was observed in the Schaefer-Bergmann pattern obtained by shear waves in the (001) plane. The highest intensity was attained along [110] and the intensity became weak rapidly as the direction of the sound propagation approached [100]. A qualitative explanation of the intensity variation taking account of the corresponding figures of merit, 793×10^{-18} along [110] and 1.76×10^{-18} sec³/g along [100] is given.

Among several acoustic modes in TeO_2 , two modes are found to be particularly interesting in acousto-optical applications referring to the table and attenuation characteristics shown in Fig. 2; one is the shear mode propagated in the [110] direction with displacement along $[\bar{1}10]$ and the other is the longitudinal mode along [001]. The former produces light diffraction with the highest efficiency hardly observed in most solids, though the usable frequency range will be restricted below 100 MHz, because of rapid increase in sound attenuation with frequency. Calculation shows that an acoustic power of only 260 mW is required for 100% deflection of incident 6328 Å light when a cross section of the acoustic beam is a square. The latter mode is also preferable for the applications because of the fairly high M , remarkably high M' , and relatively small acoustic absorption. The comparably low acoustic loss will make it possible for the crystal to be used up to about 1 GHz when a thermal effect due to the loss is adequately treated. More detailed studies will be necessary for designing the devices, including temperature dependence of sound velocity, acoustic loss, and figure of merit as well as the dispersion characteristics of the acousto-optical behavior, which are now under investigation.

ACKNOWLEDGMENTS

The authors are greatly indebted to S. Miyazawa, without whose efforts for preparing the single crystals the present study would never have been carried out. Several helpful discussions with N. Niizeki and H. Iwasaki are also gratefully acknowledged.

²⁹ N. Uchida, Japan. J. Appl. Phys. **8**, 329 (1969).

³⁰ E. I. Gordon, IEEE J. Quant. Electron. **2**, 104 (1966).

³¹ N. Uchida, Japan. J. Appl. Phys. **7**, 1259 (1968).